ScienSage

Journal of Advanced Scientific Research

Available online through http://www.sciensage.info

ISSN
0976-9595
Research Article

STUDIES OF MAGNESIUM DOPED MnS NANOMATERIAL SYNTHESIZED BY MICROWAVE-ASSISTED SOLUTION METHOD

K. Jeyamalar*[1], P. Selvarajan[2]

[1]*Research scholar, Department of Physics, Bharathiar University, Coimbatore, Tamilnadu, India*

[2]*Department of Physics, Aditanar College of Arts and Science, Tiruchendur, Tamilnadu, India*

**Corresponding author: ajeyamalar75@gamil.com*

ABSTRACT

Manganese sulfide (MnS) is a wide band gap material which has the potential use in short wavelength optoelectronic devices, photo-catalysis, solar cells etc. To alter the various properties of MnS nanomaterial, it was decided to add magnesium (Mg) as the dopant. Mg-doped MnS nanomaterial was synthesized by microwave-assisted solution method. From XRD and HRTEM studies, the crystallite size of the sample was estimated. Optical characterization of the sample was done by recording the UV-visible-NIR spectrum. The luminescent properties of Mg-doped MnS nanomaterial was analysed. The functional groups of the sample was found by FTIR studies and thermal stability was checked by TG/DTA studies. Also, Mg-doped MnS nanomaterial was characterized by SEM, EDAX and SAED studies.

Keywords: Nanomaterial Doping, XRD, HRTEM, SEM, FTIR, Photoluminescence, SAED, Optical absorption, TG/DTA.

1. INTRODUCTION

Manganese sulfide (MnS) is an important semiconductor material which has three forms: α-MnS, β-MnS and γ-MnS forms. The α-MnS form crystallizes in cubic structure and it is an antiferromagnetic material with a Neel temperature at 150 K. The β-MnS form crystallizes in zinc blende structure and γ-MnS form has the wurtzite structure [1-4]. MnS is a wide band gap semiconductor that has a potential use in short wavelength optoelectronic devices such as in solar selective coatings, solar cells, sensors, photoconductors, optical mass memories as well as like a blue green light emitter [5-10]. It is reported that doping is one of the common methods to alter electrical, optical and magnetic properties of nanomaterials and hence the researchers have doped materials like MnS and ZnS with metal ions [11-14]. Dae Sung Kim et al. have synthesized Cd-doped α-Mns nanowires by the chemical vapor deposition. XRD analysis indicates that Cd-doping changes the lattice parameters by 0.3% and photoluminescence property and band gap of the sample have been altered due to doping [15]. Shahid et al. have reported that band gap tunability of ZnS is possible by doping of impurities like Mg and Mn and they analyzed the theoretical model based on first principle theory using local density approximation and here also Mg-doped ZnS nanomaterial was studied by XRD, SEM, FTIR, EDS, UV-Vis and Hall measurements [16]. Pradeev Raj et al. used co-precipitation method to synthesize pure and Mg-doped ZnO nanoparticles and the structure, morphology, chemical composition, and optical and antibacterial activity of the sample were carried out. It is found that band gap energy of ZnO sample was altered with an increase in Mg doping concentration [17]. Based on the literature survey, it is planned to add magnesium (Mg) as the dopant into the host MnS nanomaterial to modify its various properties. Hence, the aim of the work is to synthesize Mg-doped manganese sulfide (MnS) nanoparticles by microwave-assisted solution method and to carry out structural, optical, FTIR, SEM, TEM, SAED, EDAX and photoluminescence studies for the synthesized nanomaterial.

2. MATERIAL AND METHODS

2.1. Reactants

Manganese acetate, thiourea, magnesium chloride, L-tartaric acid and sodium hydroxide etc were used.

2.2. Synthesis

AR chemicals such as manganese acetate and thiourea (Merck India) were taken in 1:1 molar ratio and they

were dissolved the double distilled water in a borosil beaker. The chemicals were used as received. 10 mole% of magnesium chloride was added into the prepared solution. Using a magnetic stirrer, the solution was stirred for 1 hour. During the stirring, 0.5 M aqueous solution of sodium hydroxide was added to increase the pH value to 10. After stirring, the solution was kept in a domestic microwave oven (900 W, 2450 MHz. Onida, India). The apparatus was fully loaded with rotating hard glass circular plate at the bottom to place the bowl on it. The side wall of the apparatus was well protected with tin sheet cover. The solution was placed inside the bowl with top cover which was sustainable for the heat produced inside the oven. The solution was subjected to microwave irradiation of 900 W for 30 minutes. The colloidal precipitate obtained after this irradiation was air cooled to room temperature. The material was washed several times using doubly distilled water and then with acetone to remove the unwanted impurities. Using a furnace, the conventional thermal treatment was carried out for the prepared sample at 400°C in air for 7 hours. Then, the powder nanosample of Mg-doped MnS was subjected to various studies like powder XRD studies using the powder X-ray diffractometer, SEM and EDAX studies using the scanning electron microscope, FTIR studies using the FTIR spectrometer, optical studies using the UV-visible spectrophotometer, TEM studies using the transmission electron microscope, PL studies using the photoluminescence spectrometer.

3. RESULTS AND DISCUSSION

3.1. EDAX and SEM studies

Energy dispersive X-ray spectroscopy (EDS or EDAX) is an analytical technique used for identifying the chemical composition of a sample. It is known that interaction of an electron beam with the sample produces a variety of emissions, including X-rays and this principle is used in both EDAX and SEM. In EDAX method, an energy dispersive detector is used to separate the characteristic X-rays of different elements into an energy spectrum and using this spectrum, different elements of the sample can be identified. EDAX spectrum and SEM images of Mg-doped MnS nanomaterial were recorded at STIC, Cochin University, Cochin using an Scanning Electron Microscope with Energy dispersive X-ray spectroscope (SEM-EDAX, Model: Jeol 6390LA/ OXFORD). The recorded EDAX spectrum of the sample is shown in the fig. 1 and from this spectrum, the elements such as Mg, Mn and S have been identified. The weight and atomic percentage of the elements in Mg-doped MnS material are provided in the table 1. The SEM image with magnification x 1500 of Mg-doped MnS nanomaterial is shown in the fig. 2 and SEM image with magnification x 3500 of the sample is depicted in the fig. 3. From the SEM images, it is observed that some particles are in spherical shapes and other particles are irregular shapes and elongated. Also it is seen that many particles are agglomerated.

Table 1: Weight percentage and atomic percentage of various elements in Mg-doped MnS nanomaterial

Element	Weight percentage	Atomic percentage
Mn	62.84	54.35
S	34.68	42.74
Mg	2.47	2.88

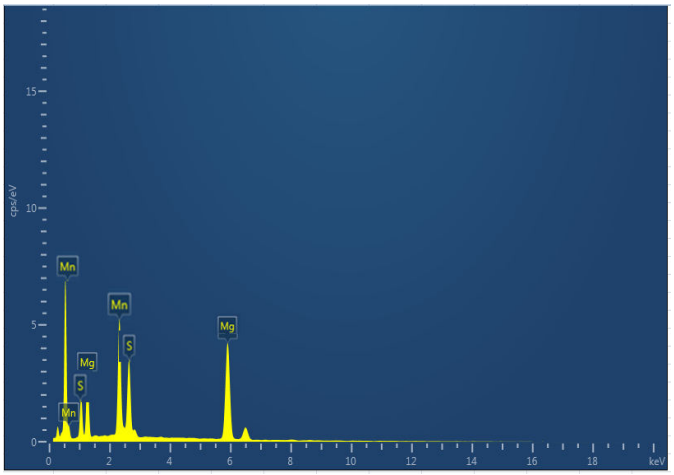

Fig. 1: EDAX spectrum of Mg-doped MnS nanomaterial

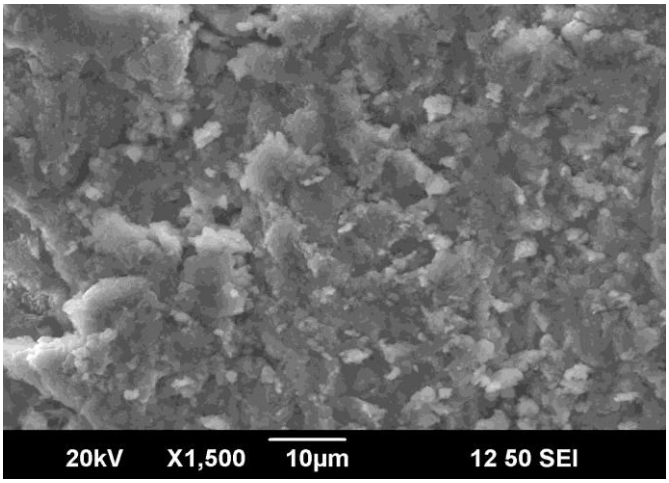

Fig. 2: SEM image (magnification x 1500) of Mg-doped MnS nanomaterial

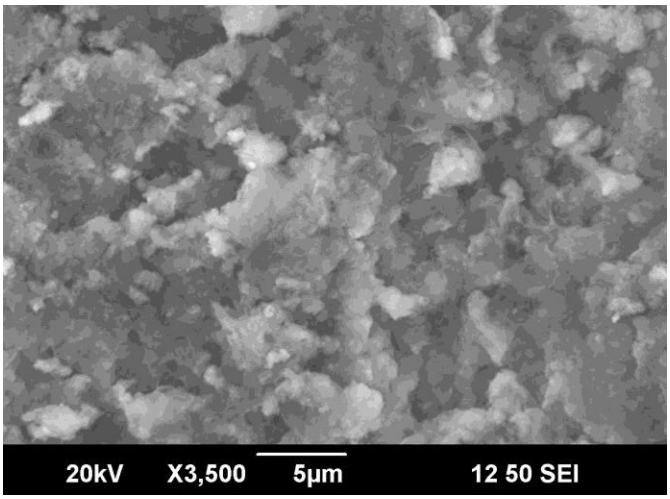

Fig. 3: SEM image (magnification x 3500) of Mg-doped MnS nanomaterial

3.2. Optical characterizaiton

Optical absorption spectrum for Mg-doped MnS nanoparicles were recorded in the wavelength range from 200-1900 nm and it is shown in the Fig. 4. The prepared sample was ultrasonically dispersed in acetone and for the liquid sample, the spectrum was recorded using the UV-Vis-NIR spectrophotometer (Agilent Cary 5000) in the absorption mode. Here pure acetone was used as the reference sample. This spectrum contains three regions viz. UV region, visible region and IR region and a broad absorption peak at 368 nm is observed in the UV region and this wavelength is the UV absorption edge wavelength. The absorption is high in UV region and it is low in the visible region. It is to be mentioned here that the UV spectrum of the sample was recorded upto 1900 nm and it contains a small absorption peak at 1400 nm and high absorption is seen at 1850 nm. Also this spectrum contains some spikes around 800 nm and this may be due to impurities in the sample. This result is similar to the work of other researchers [18, 19]. The optical band gap of the sample was determined using the relation $E_g = 1240/\lambda$ where λ is the UV absorption edge wavelength or cut-off wavelength and the obtained value is 3.37 eV. This bandgap value is slightly more than that of bulk MnS material (E_g =3.3 eV) which indicates that the blue shift arises due to quantum size effect. Compared to undoped MnS nanomaterial (E_g = 3.444 eV), the band gap Mg-doped nanomaterial is slightly less and this may due to formation of dopant levels in between the valence band and conduction band [20].

The transmittance value of the sample was calculated using the relation $A = \log_{10}(1/T)$ where A is the absorbance and T is the transmittance. The transmittance spectrum of 'Mg-doped MnS nanomaterial dispersed in acetone' was presented in the fig. 5 and it shows the high transparency of the sample in the IR region. Using the values of transmittance, the linear absorption coefficient value is calculated using the relation $\alpha = (2.303 \log(1/T))/t$ where 't' is the thickness of the sample. The variation of absorption coefficient with wavelength for Mg-doped MnS nanomaterial is shown in the fig. 6 and this behaviour is similar to the plot of absorbance versus wavelength plot (Fig. 2). The value of reflectance of the sample is determined using the relation $R = 1 \pm (1-\exp(-\alpha t)+\exp(\alpha t))^{1/2}/(1+\exp(-\alpha t))$. The plot of reflectance versus wavelength for Mg-doped MnS nanomaterial is shown in the fig. 7 and indicates that reflectance is low in UV-visible regions and it is high in the IR region. The negative values of reflectance in the UV region and visible regions indicate that the sample can be used for anti-reflection coatings. Using the values of absorption coefficient, the extinction coefficient was determined using the equation $K = \alpha\lambda/4\pi$ where λ is the wavelength of light. When an electromagnetic wave propagates through a sample, there will be energy loss and it is given by extinction coefficient [21]. The plot of extinction coefficient versus wavelength for Mg-doped MnS nanomaterial is presented in the fig. 8. The result indicates that the sample has low extinction coefficient of the order of 10^{-5} and it increases as the wavelength increases and in the IR region, its value is high.

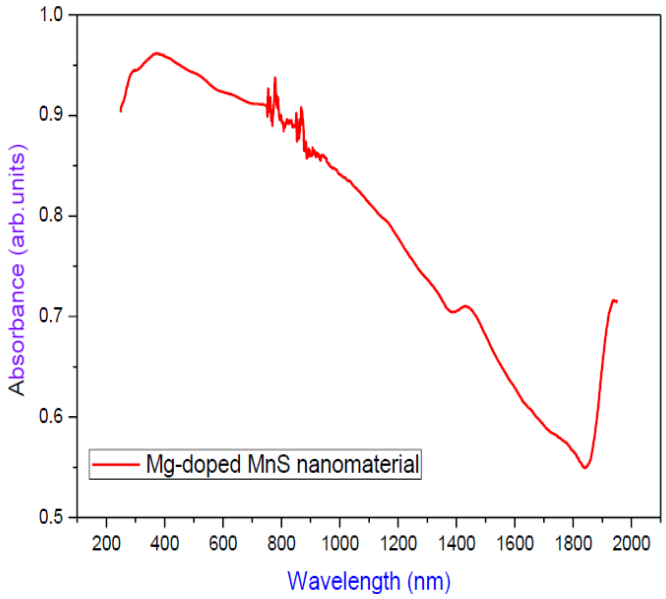

Fig. 4: Absorbance spectrum of Mg-doped MnS nanomaterial

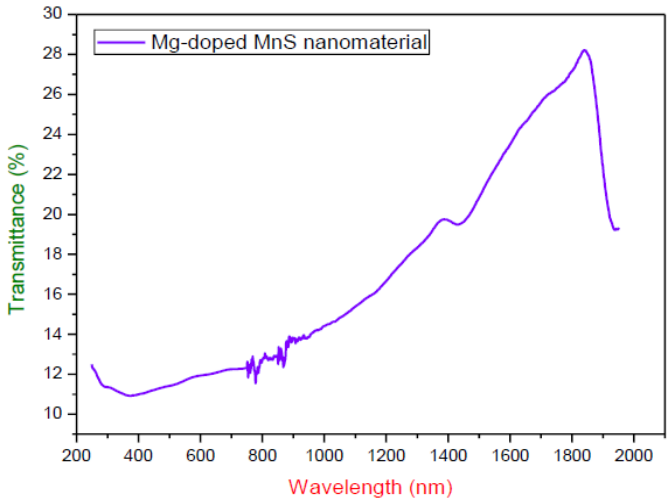

Fig. 5: Transmittance spectrum of Mg-doped MnS nanomaterial

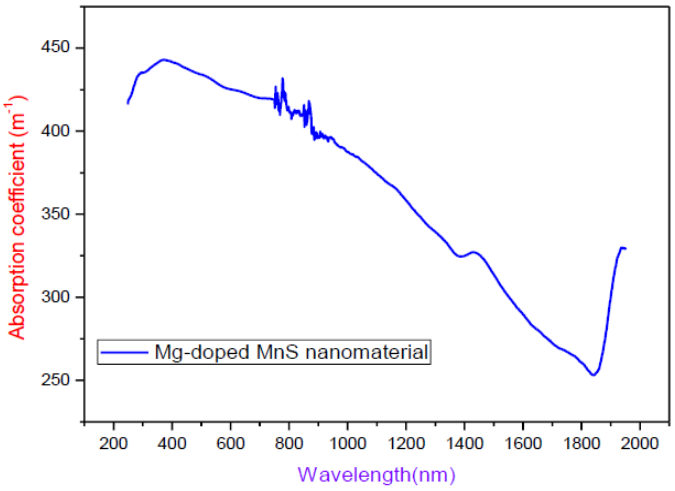

Fig. 6: Variation of absorption coefficient with wavelength for Mg-doped MnS nanomaterial

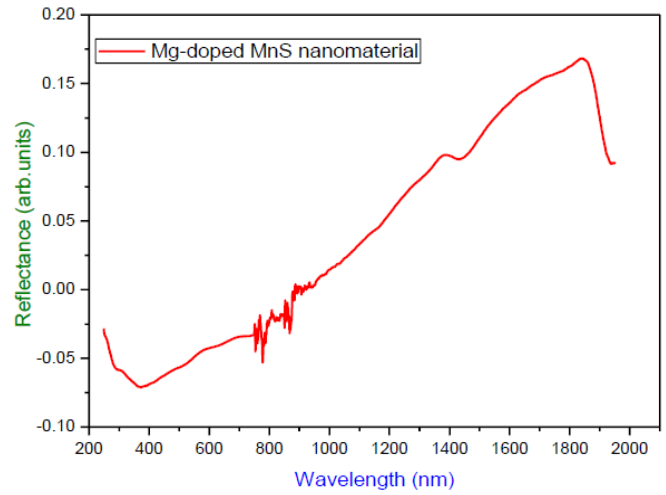

Fig. 7: Reflectance spectrum of Mg-doped MnS nanomaterial

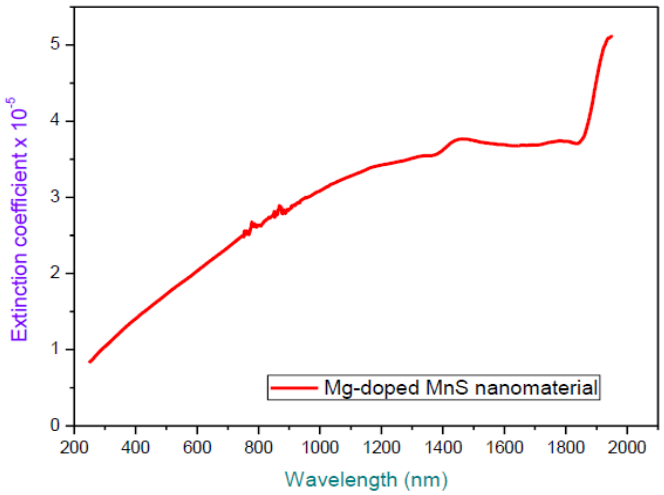

Fig. 8: Plot of extinction coefficient versus wavelength for Mg-doped MnS nanoparticles

3.3. Powder XRD studies

The crystalline structures of the new materials are found using single crystal diffractometer whereas powder diffractrometer are used for phase identification and quantitative phase analysis. The diffraction methods are based on generation of X-rays in an X-ray tube and these X-rays are directed onto the sample to measure the intensity of diffracted rays. From the intensity and two-theta values, crystal structure of the sample will be solved. Powder XRD study is used to analyze the crystalinity, paricle size, phase of the sample. The powder XRD pattern of Mg-doped MnS nanomaterial was recorded in Cochin University using the powder XRD diffractometer (Mode: Bruker D8 Advance, Copper target, Nickel filter) in the two-theta range of 10°-80° and the recorded XRD pattern is shown in the fig. 9. The XRD pattern contains many broadened diffraction peaks and hence it indicates that the prepared material is a nanosample. The diffraction peaks can be indexed to the cubic MnS material (JCPDS card No. 06-0518) [1]. The peaks at two-theta values of 31.56°, 36.36°, 45.42°, 52.85°, 60.71°, 64.44° and75.44° are corresponding to the (hkl) vaues of (111), (200), (220), (311), (222), (400), (331) and (420) respectively. Some additional diffraction peaks are also noticed in the pattern and these are due to doping of magnesium into the lattice of MnS nanomaterial. The crystallite size of the Mg-doped MnS nanomaterial was determined using the Scherrer's formula $D=0.9\ \lambda/\beta\ \cos\theta$ where β is full width a half maximum, λ is the wavelength of X-rays and θ is the Bragg's angle. The average crystallite size of the sample was found to be 15.47 nm.

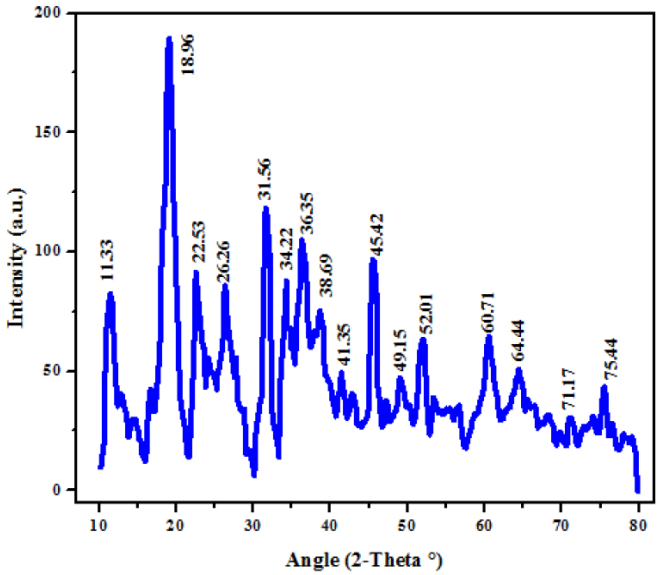

Fig. 9: Powder XRD pattern of Mg-doped MnS nanomaterial

3.4. HRTEM and SAED studies

Transmission electron microscopy (TEM) is a technique that uses the interaction of energetic electrons with the sample and provides morphological and compositional information. But the high-resolution transmission electron microscopy (HRTEM) uses both the transmitted and the scattered beams to create an interference image. It is a phase contrast image and can be as small as the unit cell of crystal. HRTEM has been extensively and successfully used for analyzing crystal structures, lattice imperfections and nanomaterials on an atomic resolution scale. The morphology and particle size of Mg-doped MnS nanomaterial were investigated using the HRTEM (Model: Jeol/JEM 2100) at Cochin University, Cochin and the figs. 10 and 11 show HRTEM images of the sample in different resolutions such as 20 nm and 50 nm. Fig. 8 shows the nanoparticles of different sizes like 12.87 nm, 11.95 nm, 8.95 nm, 14.85 nm, 9.19 nm and 12.56 nm. Hence, the average particle size is obtained to be 11.73 nm. This value is comparable to that obtained by XRD studies. Fig.9 shows the sample contains some elongated, spherical and irregular nanostructures. The selected area electron diffraction (SAED) pattern on a single Mg-doped MnS nanoparticle is presented in the fig. 10 and it displays a set of diffraction rings and each ring contains many spots. The spots on the pattern indicate that each nanoparticle is a single crystal. Each spot on the ring represents a crystal plane and all the spots on a ring represent a group of parallel planes having same Miller indices. Hence, the three rings on SAED pattern can be assigned to {111}, {200} and {220} planes of cubic crystal structure [22].

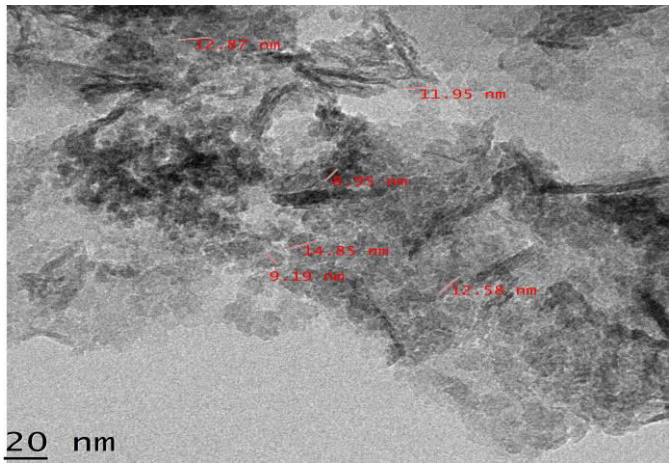

Fig. 10: HRTEM image of Mg-doped MnS nanomaterial with the resolution of 20 nm

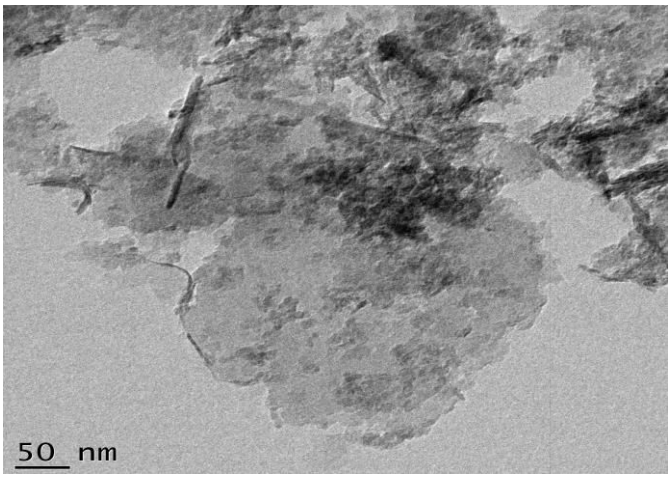

Fig. 11: HRTEM image of Mg-doped MnS nanomaterial with the resolution of 50 nm

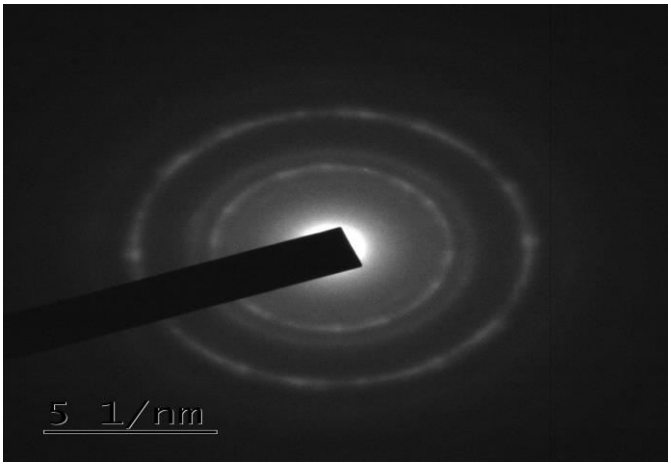

Fig. 12: SAED pattern for Mg-doped MnS nanoparticle

3.5. PL studies

Photoluminescence (PL) is the phenomenon in which electronic states of a solid are excited by light of particular energy and the excitation energy is released as light. Usually, the sample is excited with UV light and the emitted light is observed to be in UV, visible and infrared regions. The PL spectrum of Mg-doped MnS nanomaterial was recorded using a Fluorolog-3 spectrofluorometer (HORIBA JOBIN YVON) with a Xenon lamp as the excitation source. In this experiment, the excitation wavelength used is 240 nm and the recorded PL emission spectrum is shown in the fig. 13. The PL spectrum of Mg-doped MnS nanomaterial consists of three significant peaks at 360 nm, 374 nm and 494 nm. When the sample absorbs UV light at wavelength of 240 nm, the electrons are excited from valence band to higher excitation bands and when they return to lower energy states, UV and visible radiations are emitted. Here, the UV emission peaks noticed are at 360 nm and 374 nm and the visible emission peak is at 494 nm. The spectrum also consists small emission peaks which are corresponding to magnesium dopant into MnS nanomaterial. Similar results for other materials have also been published in the journals [23-25].

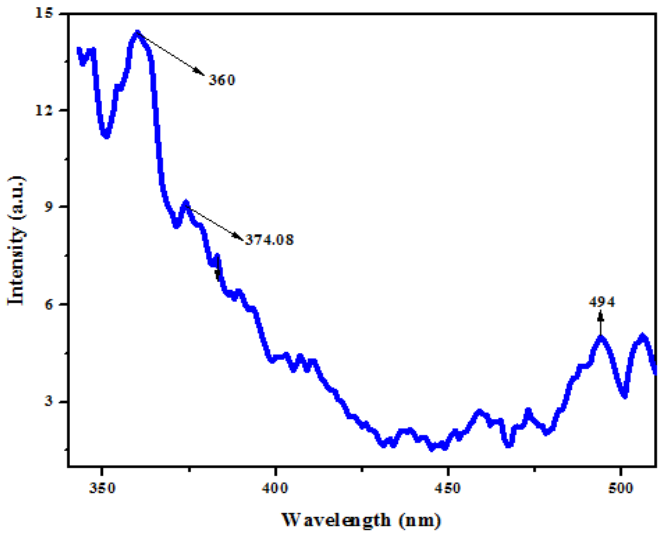

Fig. 13: PL spectrum of Mg-doped MnS nano-material

3.6. Theraml studies

The thermal stability of Mg-doped MnS nanomaterial was checked by TG/DTA studies and these studies were carried out using a NETZSCH STA 409C/CD thermal analyzer in nitrogen atmosphere in the temperature range 30-850°C. The recorded TG/DTA curves of the sample are presented in the fig. 14 and to point out different stages of decomposition, the TG curve is shown in the separate fig. 15. There are three stages in the TG curve and in the first stage (30-120°C), there is a loss of about 23 weight% of the sample and this is due to loss of adsorbed water molecules. In the second stage (120-380°C), the sample decomposes and there is a weight loss of about 25%. In the third stage (380-850°C), the weight loss noticed is very less (about 3%). From the DTA curve, the slightly broad endothermic peak at 100°C represents the removal of adsorbed water molecules. The two exothermic peaks at 360°C and 380°C indicate the decomposition of the sample. The two peaks are corresponding to the decomposition of two types of the chemicals in the sample.

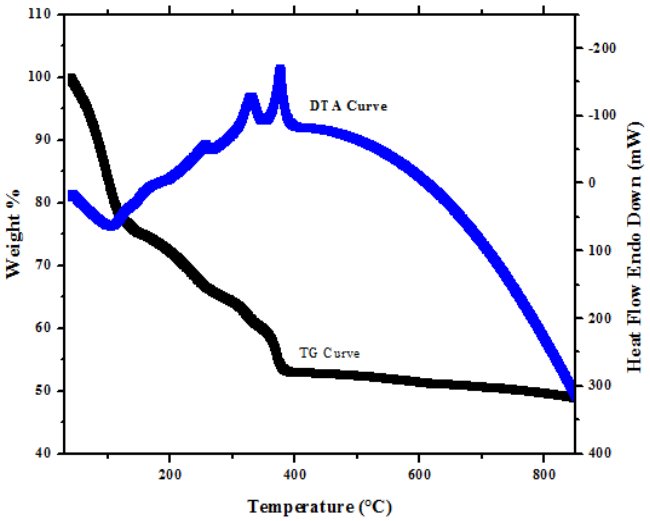

Fig. 14: TG/DTA thermal curves for Mg-doped MnS nanomaterial

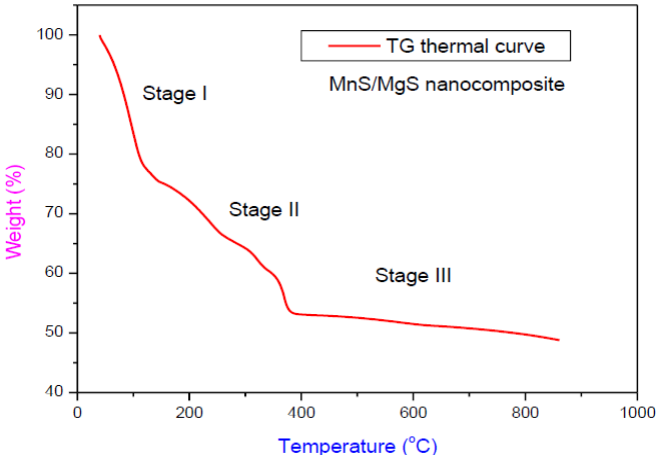

Fig. 15: TG curve of Mg-doped MnS nanomaterial shown different stages of decomposition

3.7. FTIR studies

The functional groups of Mg-doped MnS nanomateial have been identified by Fourier transform infrared (FTIR) studies. This study was carried out using an FTIR spectrometer (Model: Thermo Nicolet Avtar 370 4000) in the wave number range 400-4000 cm^{-1}. When the frequency of the infrared radiation coincides with the vibrational frequency of some part of the molecule of a sample, resonance occurs and absorption of energy takes place. When the molecules returns from the excited state to the original ground state, the absorbed energy is released which results in distinct peaks in the spectrum. Compared to IR spectrum, the FTIR spectrum has high resolution and hence FTIR spectrum of the sample has been recorded. The FTIR spectrum of Mg-doped MnS nanomaterial is shown in the fig. 16. The broad absorption peak at 3415 cm^{-1} is corresponding to OH stretching vibration of adsorbed water molecules (moisture) from the atmosphere. The absorption peaks at 2919 cm^{-1} and 2847 cm^{-1} due to CH stretching and these peaks are insignificant in the spectrum. The bending vibrations of OH are found at 1626 cm^{-1} and at 1439 cm^{-1}. Due to absorption of moisture by the sample, OH stretching and bending vibrations are occurring [26]. The absorption peaks at 615 and at 430 cm^{-1} are due to Mn-S stretching vibrations as reported in the literature [27].

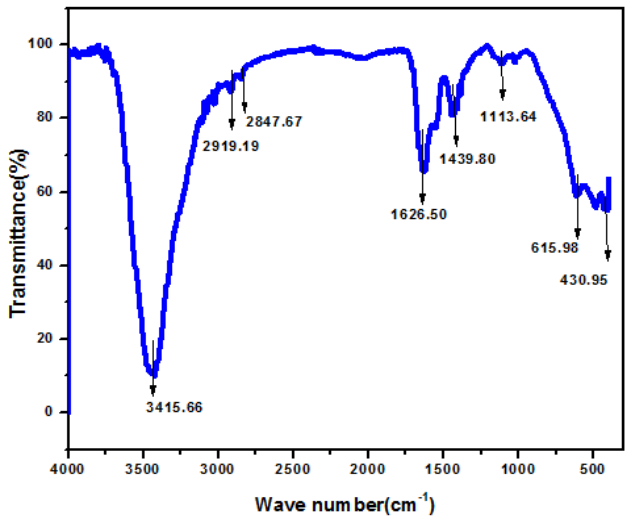

Fig. 16: FTIR specrum of Mg-doped MnS nano-material

4. CONCLUSION

Microwave oven was used to prepare Mg-doped MnS nanomaterial and thiourea was used as the source of sulphur. The nanoparticles crystallize in cubic structure and hence the formed material belongs to α-MnS doped with magnesium. UV-visible spectrum of the sample was recorded and linear optical parameters like transmittance, absorbance, reflectance, absorption coefficient and extinction coefficient were analysed. HRTEM image and SAED pattern of the sample was taken and particle size was evaluated and the nanoparticle is confirmed to be single crystalline in nature. EDAX method was used to find the weight percentage and atomic percentage of various elements in Mg-doped MnS nanomaterial. The morphology of the particles was analysed by SEM studies. FTIR study indicates that this sample absorbs water molecules from moisture. The thermal stability of the prepared material was tested by TG/DTA studies. From photoluminescence study, it is confirmed that Mg-doped MnS nanomaterial emits UV and visible light when it was excited with 240 nm. Since the band gap of MnS nanomaterial is changed when magnesium is doped, the band gap of the sample can be tunable by adding different concentration of the dopant and antibacterial activity and magnetic studies of this sample could be carried out in the future.

5. AKNOWLEDGEMENT

The authors are thankful to the staff members of STIC, Cochin Univeristy (Cochin) and St.Joseph's College (Trichy) for collecting the data to carry out the research work.

Conflict of interest

None declared

6. REFERENCES

1. Biswas S, Kar S, Chaudhuri S. *J.Crystal Growth,* 2005; **284:**129-135.
2. Cheng Y, Wang Y, Jia C, Bao F. *Journal of Physical Chemistry B,* 2006; **110:**24399-24402.
3. Zhang Y, Wang H, Wang B, Yan H, YoshimuraM. *J.Crystal Growth,* 2002; **243:**214-217.
4. Zuo T, Sun Z, Zhao Y, Jiang X, Gao X. *Journal of the American Chemical Society,*2010; **132:**6618-6619.
5. Fan D, Wang H, Zhang Y, Cheng J, Wang B, Yan H. *Surf. Rev.Lett.,* 2004; **11:**27-31.
6. Pandey G, Sharma HK, Srivastava SK, Srivastava RK, Kotnala RK. *Mater.Res.Bull.,* 2011; **46:**1804-1810.
7. Ulutas C, Guneri E, Kirmizigul F, Altindemir G, Gode F, Gümüs C. *Mater.Chem.Phys.,* 2013; **138:**817-822.
8. Tappero R, D'Arco P, Lichanot A. *Chem.Phys.Lett.,* 1997; **273:**83-90.

9. Fan D, Yang X, Wang H, Zhang Y, Yan H, *Phys. B,* 2003; **337:**165-169.
10. Dhasade SS, Patil S, Rath MC, Fulari VJ. *Mater.Lett.,* 2013; **98:** 250-253.
11. Kim DS, Lee JY, Na CW, Yoon SW, Kim SY, Park J, Jo Y, Jung MH. *The Journal of Physical Chemistry B,* 2006; **110:**18262-18266.
12. Zhang N, Yi R, Wang Z, Shi R, Wang H, Qiu G, Liu X. *Materials Chemistry and Physics,* 2008; **111:**13-16.
13. Shehab AA, Fadaam SA. *Journal of Multidisciplinary Engineering Science and Technology,* 2016; **3:**5577-5583.
14. Veeramanikandasamy T, Rajendran K, Sambath K, Rameshbabu P. *Materials Chemistry and Physics,* 2016; **171:** 328-335.
15. Dae Sung Kim, Jin Young Lee, Chan Woong Na, Sang Won Yoon, Shin Young Kim, Jeunghee Park et al. *J.Phys.Chem. B,* 2006; **110:** 18262-18266.
16. Shahid MY, Asghar M, Arbi HM, Zafar M, Ilyas SZ. *AIP Advances,* 2016; **6:** 025019.
17. Pradeev Raj K, Sadaiyandi K, Kennedy A, Suresh Sagadevan, Zaira Zaman Chowdhury, Mohd. Rafie Bin Johan, et al. *Nanoscale Research Letters,* 2018; **13:**229-236.
18. Lokhande CD, Ennaoui A, Patil PS, Giersig M, Muller M, Diesner K, Tributsch H. *Thin Solid Film,* 1998; **330:**70-75.
19. Sunil H, ChakiMP, DeshpandeJP, TailorKS, Mahato MD, Chaudhary, *Advanced Materials Research,* 2012; **584:**243-247.
20. Jeyamalar K, Selvarajan P. *Int. J. Adv. Trends in Eng. Tech.* 2018; **3:**104-111.
21. Hanumantharao R, Bhagavannarayana G, Kalainathan S. *Spectrochim.Acta* 2012; **A91:**345-351.
22. Xinhua Z, Yiqing C, Chong J, Qingtao Z, Yong S, Bo P, Song Y, Minjun X. *Materials Letters,* 2008; **62:**125-127.
23. Luo YS, Zhang WD, Dai XJ, Yang Y, Fu YS. *J.Phys. Chem.,* 2009; **C113(12):**4856-4861.
24. Dai XJ, Luo YS, Fu SY, Chen WQ, Lu Y. *Solid State Sci.,* 2010; **12(4):**637-642.
25. Wallick GC. *Phy.Rev.,* 1951; **84(2):**375-381.
26. Wang TX, Chen WW. *Chem. Eng. J.,* 2008; **144:**146-148.
27. Liu JD, Zheng XS, Shi ZF, Zhang SQ. *Ionics, 2014;* **20:**659-664.